Taiwan Journal of Ophthalmology 6 (2016) 8–14

Contents lists available at ScienceDirect

Taiwan Journal of Ophthalmology

journal homepage: www.e-tjo.com

Review article

Retinal complications associated with congenital optic disc anomalies determined by swept source optical coherence tomography☆

Makoto Inoue*

Kyorin Eye Center, Kyorin University School of Medicine, Tokyo, Japan

ARTICLE INFO

Article history:
Received 8 April 2015
Accepted 20 May 2015
Available online 15 July 2015

Keywords:
coloboma
congenital optic disc anomaly
morning glory syndrome
optic disc pit
optical coherence tomography

ABSTRACT

Optical coherence tomography has evolved over the past 2 decades to be an important ancillary method to evaluate diseases of the anterior and posterior segments of the eye. The more recent development of swept-source optical coherence tomography (SS-OCT) with a wavelength-tunable laser centered at 1050 nm and deeper imaging depth of 2.6 mm has enabled clinicians to evaluate congenital optic disc anomalies including optic disc pits, optic disc colobomas, and morning glory syndrome in more detail. The SS-OCT findings of the posterior precortical vitreous pocket, Cloquet's canal, lamina cribrosa that is torn from the peripapillary sclera, and the retrobulbar subarachnoid space immediately posterior to the highly reflective tissue lining the bottom of the excavation are presented. In addition, abnormal communications between the vitreous cavity and the subretinal and subarachnoid spaces in eyes with congenital optic disc anomalies are also reviewed. The retinal complications associated with congenital optic disc anomalies are treated by vitreous surgery, silicone oil tamponade, and peripapillary laser photocoagulation or scleral buckling. However, the surgical outcomes are limited and not entirely satisfactory. Analyses by SS-OCT of congenital optic disc anomalies should make the treatment correspond better with the pathological findings.

1. Introduction

Congenital optic disc anomalies consist of optic disc pits, optic disc colobomas, the morning glory syndrome, optic nerve aplasia or hypoplasia, and peripapillary staphylomas.[1–5] Congenital optic disc pits are anomalies of the optic nerve head and are commonly associated with retinoschisis and serous retinal detachment.[3–5] Other optic disc anomalies are associated with serous or rhegmatogenous retinal detachment. Optical coherence tomography (OCT) studies of eyes with optic disc pit maculopathy show the presence of double-layer detachments consisting of an inner layer retinoschisis and an outer layer detachment.[6] It has not yet been determined whether the fluid in the retinoschisis originates from the vitreous cavity or from leakage of cerebrospinal fluid through the peripapillary subarachnoid space.[4]

OCT has evolved over the past 2 decades to be an important ancillary method to evaluate the anterior and posterior segments of eyes with ocular diseases.[7,8] OCT is noninvasive and cross-sectional or enface images of the anterior segments, retina, choroid, and the optic nerve head can be obtained. The improved high-resolution images have enabled clinicians to obtain images that are comparable to the *in vivo* histological cross-sectional images.

Swept-source OCT (SS-OCT) is a new generation OCT that has higher penetration into the choroid and sclera.[9] SS-OCT uses a longer wavelength examination beam of around 1 μm, which allows it to examine the choroid and deeper tissues of the eye. SS-OCT can evaluate the retrobulbar subarachnoid space, vascular structures within the posterior sclera, peripapillary intrachoroidal cavitation, and orbital fat of eyes with high myopia.[10–14] The microstructures of the lamina cribrosa have been evaluated by SS-OCT in eyes with glaucomatous disc cupping in three-dimensional analyses.[15–17] We discuss the efficacy of SS-OCT in evaluating congenital optic disc anomalies.

Conflict of interest: The author has no conflict of interest concerning in this study.

☆ **Presentation**: 22th International Wu Ho-Su Memorial Congress – International Symposium of Vitreo-Retinal Diseases on August 31, 2014, Taipei.

* Kyorin Eye Center, Kyorin University School of Medicine, 6-20-2 Shinkawa, Mitaka, Tokyo 181-8611, Japan.
E-mail address: inoue@eye-center.org.

http://dx.doi.org/10.1016/j.tjo.2015.05.003

1.1. Advancement of OCT technology

The earlier OCT models used a near-infrared light source to create cross-sectional images of the retina.[7] The scanning light is divided into two pathways: a reference pathway and a sampling pathway. The sampling pathway passes through the tissue, and the light is scattered and reflected from different tissues in the retina. It is then combined with the light of the reference pathway that is reflected from a reference mirror. The interference pattern caused by the differences in coherence of the two beams is used to create axial A-scan images of the tissue at the point of the same distance to the reference mirror.[7] Thus, the reference mirror needs to move frequently to create two-dimensional tomographic images from the axial A-scan images, which is called time-domain detection.

The spectral-domain OCT (SD-OCT) system detects light echoes by simultaneously measuring the interference spectrum using an interferometer with a high-speed spectrometer instead of a moving reference mirror.[18,19] A much faster A-scan of the SD-OCT compared to time-domain OCT enables the acquisition of multiple B-scan images in a short time. Multiple B-scans from the identical retinal location are then averaged to increase the signal-to-noise ratio.[20] Image averaging makes the SD-OCT images clearer by reducing speckle noises and with a slight increase in the resolution. Enhanced depth imaging with SD-OCT can obtain images of the choroid and posterior sclera more precisely and accurately.[21,22] Enhanced depth imaging OCT images are obtained by positioning the SD-OCT device close enough to the eye to obtain an inverted image that has better contrast in deeper areas than the usual OCT images. The inverted images sharpen the continuity and enhance the retinal and choroidal features using image averaging.

SS-OCT uses another form of spectral domain detection to measure the light echoes.[9] SS-OCT employs a tunable frequency-swept laser light source, which sequentially emits various frequencies in time, and the interference spectrum is measured by photodetectors instead of a spectrometer. This technology increases the signal quality in deeper tissues by eliminating the sensitivity of the spectrometer to a higher frequency modulation, thereby improving the resolution of the choroid and posterior sclera. The SS-OCT (DRI OCT-1 Atlantis; Topcon, Tokyo, Japan) has an A-scan repetition rate of 100,000 Hz and the light source is a wavelength-tunable laser centered at 1050 nm with a 100-nm tuning range. The axial resolution is 8 μm, the lateral resolution is 20 μm, and the imaging depth is 2.6 mm.[23,24]

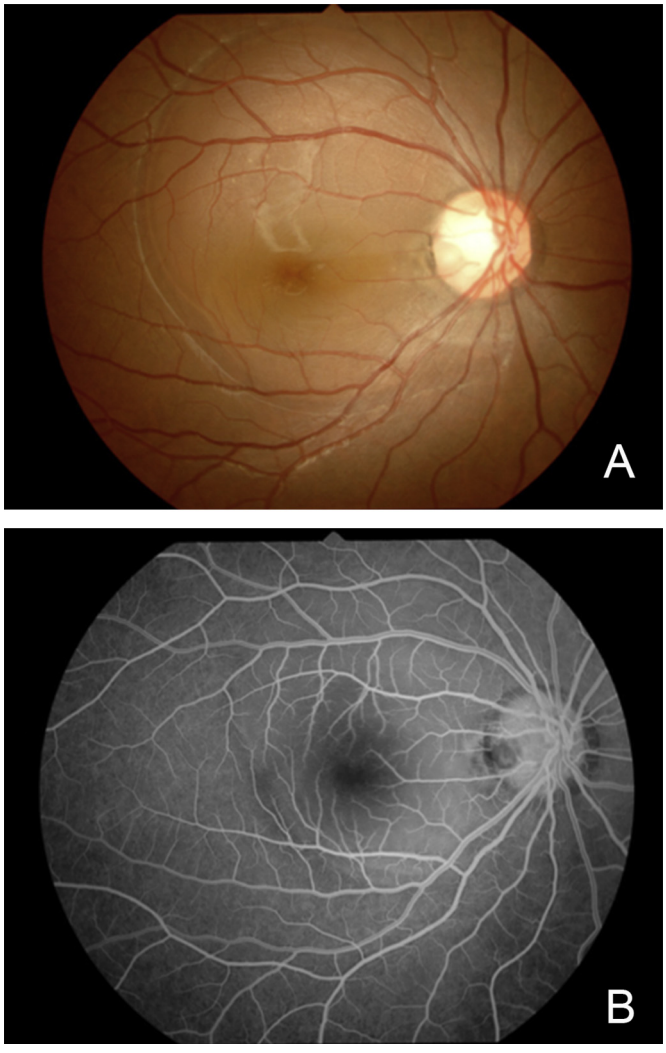

Fig. 1. Fundus photograph and fluorescein angiogram of a 17-year-old woman with optic pit maculopathy. (A) Fundus photograph showing serous retinal detachment connected to an optic pit at the temporal edge of the optic disc; (B) fluorescein angiogram in early phase shows no fluorescein leakage and hypofluorescence at the optic disc pit.

1.2. Ocular pathologies

1.2.1. Posterior precortical vitreous pocket (bursa premacularis)

A posterior precortical vitreous pocket (PPVP) is a liquefied lacuna located anterior to the macular area that is present in the vitreous of normal adults.[25] Worst[26,27] described the bursa premacularis as a pear-shaped sac with its own outer membrane, which was observed by injecting India ink into the vitreous of *postmortem* eyes. Kishi and Shimizu[25] described PPVPs in autopsy eyes, which were made visible by staining with fluorescein dye. The PPVP was considered to be the same space as the bursa premacularis except that there was no membrane but a layer of premacular cortical vitreous that adhered to the macula in young adults. PPVPs have also been identified as a dome-shaped space above the macula that can be observed during triamcinolone acetonide-assisted vitreous surgery and SD-OCT.

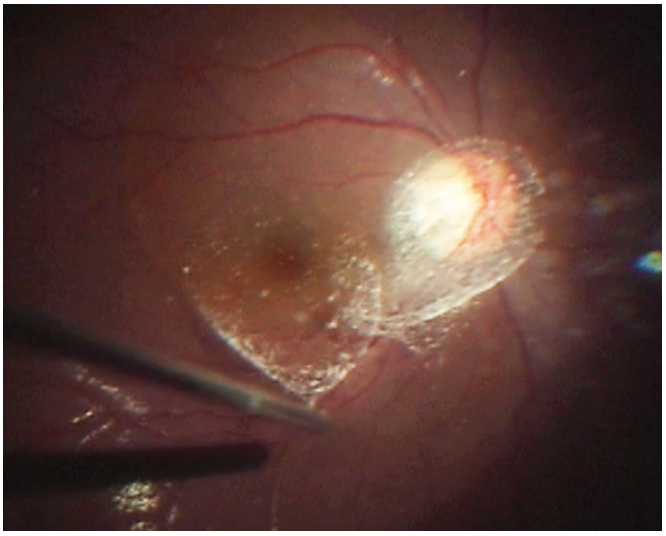

Fig. 2. Intraoperative photograph of the patient shown in Figure 1. White triamcinolone crystals can be seen in the posterior precortical vitreous pocket above the macula and Cloquet's canal above the optic disc.

The anterior border of the PPVP is vitreous gel and the posterior border is composed of a thin layer of the vitreous cortex attached to the retina. The PPVP is observed before the development of a posterior vitreous detachment. A septum is present between the nasal border of the PPVP and Cloquet's canal.[23,24] Various vitreomacular disorders including idiopathic macular holes, idiopathic epiretinal membranes, and diabetic maculopathy are known to develop by contraction or traction of the premacular vitreous cortex beneath the PPVP.[28] Highly myopic eyes are reported to have larger PPVPs than normal eyes, and partial posterior vitreous detachment (PVD) around the macula and complete PVDs occur at younger ages.[29] In eyes with a complete PVD with a Weiss ring, the vitreous cortex remains on the macula as seen in SS-OCT images in 40.5% of the eyes with high myopia which is significantly higher than that in control nonmyopic eyes at 8.7% ($p < 0.0001$).

Details of the morphological structure of PPVPs determined by SS-OCT were reported by Itakura et al.[23] The PPVPs in the SS-OCT images are boat-shaped lacunae in the macular area and are mainly bilateral in normal individuals with a mean age of 26.2 years (range, 22–40 years). The size of the PPVP measured in the SS-OCT images was: maximal width, 3114–9887 μm; mean width, 6420.6 μm; and central height, 208–1877 μm. There was a

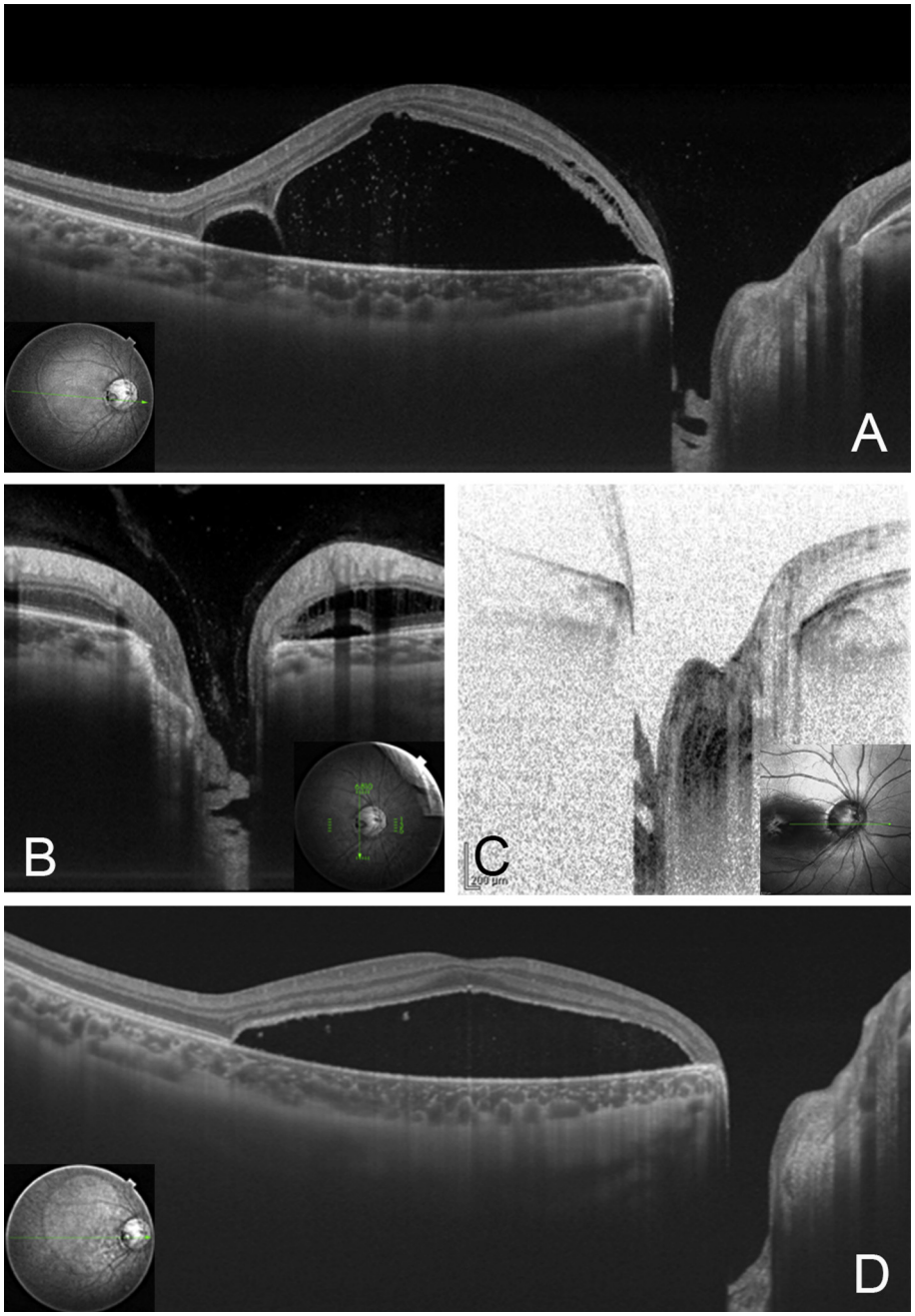

Fig. 3. Pre- and postoperative optical coherence tomography (OCT) images of the patient shown in Figure 1. (A) Preoperative oblique swept-source OCT (SS-OCT) image showing retinal detachment connected to the optic disc pit as an excavation of the optic disc. At the optic disc pit, a hole-like multilayered appearance at the bottom of the optic disc pit can be seen; (B) vertical SS-OCT images of the optic disc pit showing vitreous strands connecting to the bottom of the optic disc pit; (C) spectral domain OCT does not show precortical vitreous; (D) postoperative horizontal SS-OCT image at 7 months after vitrectomy to create a posterior vitreous detachment without laser photocoagulation around the optic disc pit shows a reduction of retinal detachment and deepened bottom of the optic disc pit without any multilayered structures.

significant correlation between the PPVP height and the myopic refractive error although the width of the PPVP was not significantly correlated with the myopic refractive error.[23] The posterior wall of the PPVP was a thin vitreous cortex, which was thinnest at the fovea. There was a septum between the nasal border of the pocket and Cloquet's canal. PPVPs were bilaterally in 93.1% of the individuals. A channel connecting Cloquet's canal and PPVP was believed to be the route of aqueous humor into the PPVP.

Yokoi et al[30] used SS-OCT to evaluate PPVPs in patients aged 1–54 years, and they reported that a PPVP was detected in all of the eyes of patients older than 10 years and in none of the eyes of patients younger than 2 years. A crack in the formed vitreous was considered to be a primitive structure of the PPVP that first develops around the age of 2 years. Between 3 years and 9 years, some of the eyes have multifocal PPVPs and cracks in the premacular vitreous. High-density remnants of regressed hyaloid vessels were occasionally observed, and the remnants were connected to the Bergmeister papilla temporally along the crack and the nasal wall of the PPVP. The PPVPs were wider horizontally than vertically. Horizontal shear stress by horizontal eye movements and the remnants of the hyaloid vessels may be related to the fragility of the premacular vitreous. Li et al[31] studied PPVPs by SS-OCT in children aged 3–11 years, and they detected PPVPs as narrow liquefied spaces along the vitreoretinal interface in the macula region at age 3 years in horizontal scan images. The mean depth of the PPVPs was 426.4 ± 38.2 μm and mean width 4834.4 ± 228.1 μm. There were significant correlations between the PPVP size and age (PPVP depth, $p < 0.001$, PPVP width, $p < 0.001$) but not with the refractive error. The PPVP and Cloquet's canal appeared as separate spaces at age 3 years. The connecting channels between the PPVP and Cloquet's canal were present after age 5 years and the PPVP developed gradually with increasing age.

1.2.2. Optic disc pit maculopathy

Optic disc pits are observed as round or oval, greyish depressions of the optic disc in different sizes.[3–5] They usually occur near the temporal margin although some may be located centrally or nasally. They can be multiple and may be bilateral. Optic disc pits are considered to have a similar pathogenesis as colobomas because they can occur simultaneously with an optic disc coloboma either in the same eye or in the fellow eye. However, they often occupy at a site that is unlikely to result from an abnormal closure of the optic fissure.[5]

Traction of the vitreous on a congenital optic disc pit has been reported to cause the development of macular retinoschisis and foveal detachments (Figures 1 and 2), and when this occurs, it is called optic disc pit maculopathy.[3,4,32,33] SS-OCT clearly showed that the precortical vitreous cortex was connected to the bottom of the optic disc pit (Figure 3). SS-OCT has an imaging depth of 2.6 mm, which is deeper than that of SD-OCT, and the entire depth of the pits from their openings to the bottom can be imaged. A lamina cribrosa that is torn from the peripapillary sclera at the site of the pits can also be seen in SS-OCT images.[34] The lamina cribrosa and retrolaminar optic nerve fibers are shifted toward the opposite side of the pit, and the retinal nerve tissue is herniated into the pit. Vitreous fibers continue into the pit along the pit wall. SS-OCT can also image the subarachnoid space immediately posterior to the highly reflective tissue lining the bottom of the excavation in eyes with optic disc pits and optic disc colobomas.[34] Katome et al[35] reported a case of optic disc pit with a connection between the vitreous cavity and the retrobulbar subarachnoid space in the SS-OCT images.

Retinoschisis and foveal detachments have been successfully treated by vitreous surgery with the creation of a posterior vitreous detachment and a gas tamponade with or without laser

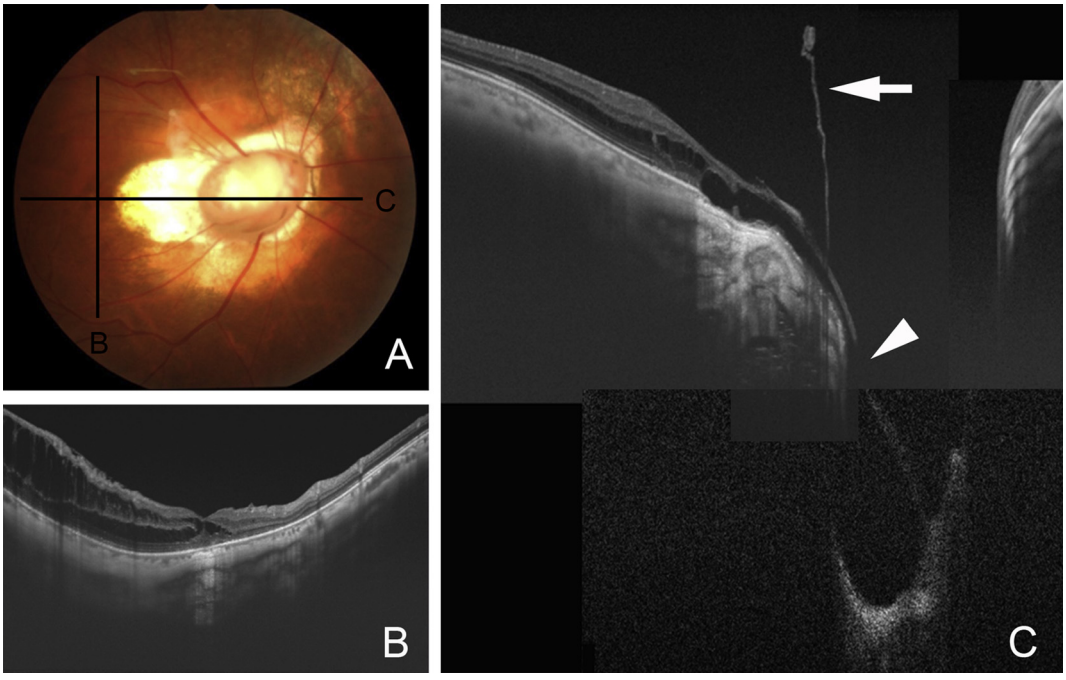

Fig. 4. Preoperative photograph and swept-source optical coherence tomography (SS-OCT) images of a 37-year-old woman with the morning glory syndrome. (A) Preoperative fundus photograph shows excavation of the enlarged optic disc with peripapillary atrophy and localized retinal detachment superior to the vascular arcade. The patient noticed a decrease of vision although the vision did not change from 0.3. Black lines indicate the scan line of the cross section of the SS-OCT images of B and C; (B) vertical SS-OCT image showing macular retinoschisis in the inner plexiform layer and outer plexiform layer; (C) montage image of horizontal sections showing detached epiretinal membrane with vitreous traction (arrow) connected to the peripapillary atrophy and retinal detachment at the excavated optic disc with a hole (arrowhead).

treatment.[36–39] The success of vitrectomy indicates that vitreous traction played some role in the development of the retinoschisis. However, in some patents with optic disc pit maculopathy, a release of vitreous traction may not be enough to resolve the retinoschisis and retinal detachment. Additional treatment with laser photocoagulation around the optic disc pit, or usage of adjuvants including serum, platelet-rich plasma, or plug of scleral autograft are recommended.[40] SS-OCT imaging can also determine whether vitrectomy alone is enough or additional treatment is required.

1.2.3. Coloboma

A congenital coloboma of the optic nerve is a cavity of different sizes at the site of the optic nerve head caused by a failure of closure of the posterior inferonasal quadrant of the embryonic fissure in the developing optic cup.[5,40] The coloboma may be unilateral or bilateral. Typical optic disc colobomas are located inferonasally and range from a large excavated disc to subtle changes in the retinal pigment epithelium. Closure of the embryonic fissure starts at the equator and extends anteriorly and posteriorly. Thus, an incomplete closure creates a coloboma of any size from the margin of the pupil to the optic disc with subtle manifestations of chorioretinal colobomas, iris, and rarely inferonasal lens defects. A rhegmatogenous retinal detachment occasionally develops in eyes with a coloboma.[41–45] Retinal holes are detected at the base of a coloboma and are difficult to treat by laser photocoagulation because of defects of the underlying retinal pigment epithelium around the holes.[42,44] Vitrectomy with photocoagulation along the coloboma border, silicone oil tamponade, planned retinotomy, or cyanoacrylate retinopexy are used to treat the retinal detachments associated with a coloboma. SS-OCT has not been used to evaluate these complications of a coloboma precisely. However, SS-OCT can detect a herniation of retinal tissue into the colobomatous area of the optic disc and subarachnoid space immediately posterior to the highly reflective tissue lining the bottom of the optic disc coloboma.[34] The herniated retina is detached from the underlying highly reflective collagenous tissue lining the bottom of the disc excavation, which may be *pia mater*.

1.2.4. Morning glory syndrome

Morning glory syndrome is a form of optic nerve coloboma characterized by a large funnel-shaped excavation of the optic nerve head and peripapillary retina.[5] The enlarged and excavated optic disc has a central glial tuft that extends anteriorly to different extents. The peripapillary area is elevated to different degrees with an associated annulus of pigment, which is most likely to represent the antecedent of a detachment. The retinal vessels emerge from the disc edge in a radial pattern and occasionally in association with

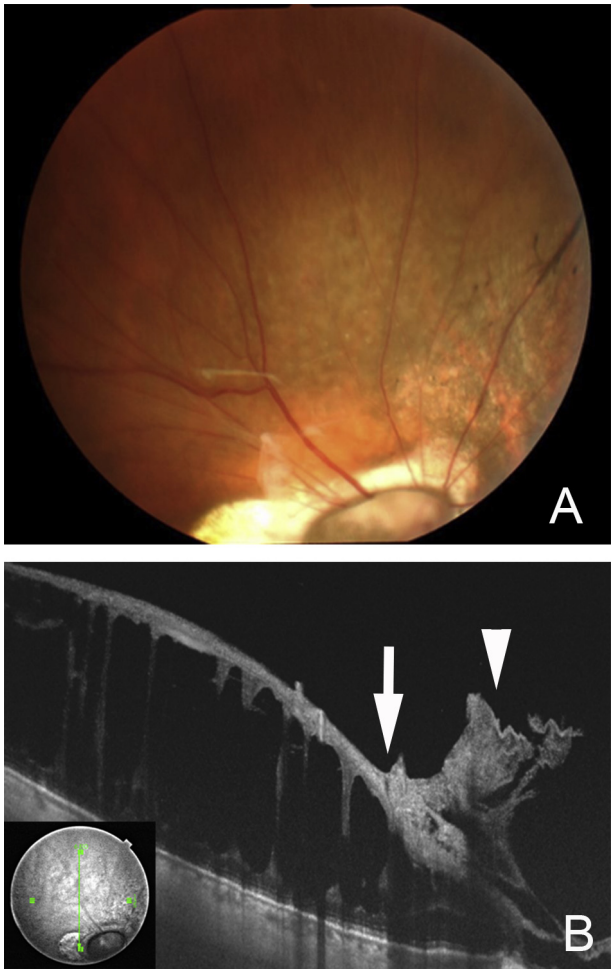

Fig. 5. Preoperative fundus photograph and swept-source optical coherence tomography images of the patient shown in Figure 4. (A) Preoperative fundus photograph showing retinoschisis and localized retinal detachment with epiretinal membrane superior to the vascular arcade; (B) swept-source optical coherence tomography image shows retinoschisis and an outer retinal hole (arrow) in conjunction with an epiretinal membrane (arrowhead).

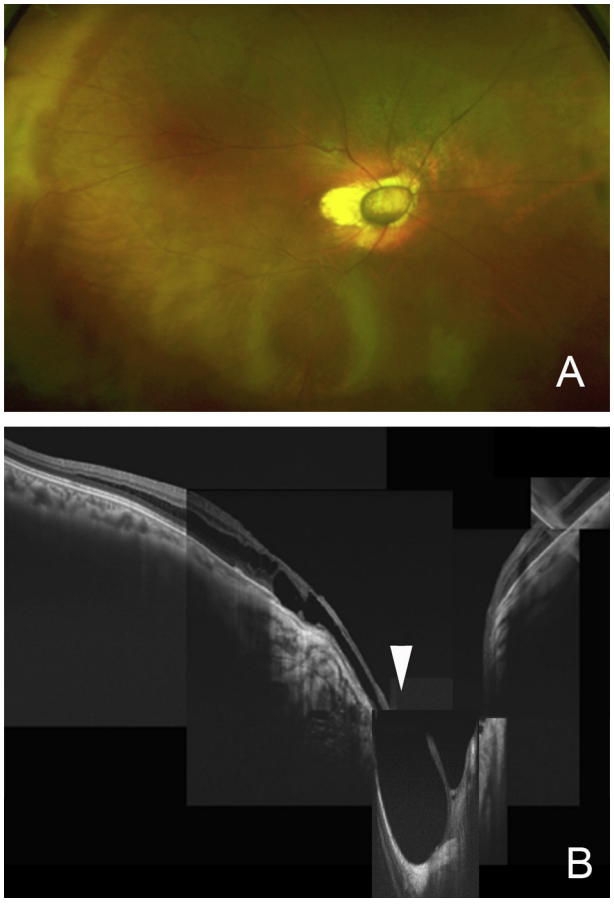

Fig. 6. Postoperative Optos image and swept-source optical coherence tomography images of the patient shown in Figure 4 at 3 months. (A) Optos ultrawide angle image shows a reduction of retinoschisis superior to the vascular arcade. Vision increased slightly to 0.4; (B) montage image of horizontal section of swept-source optical coherence tomography shows no vitreous stand while the macular retinoschisis and retinal detachment (arrowhead) at the excavated optic disc remains.

an arteriovenous shunt adjacent to or distant from the optic disc (Figures 4–7).

Cennamo et al[46] evaluated 22 eyes of 19 patients with morning glory syndrome by SD-OCT. The SD-OCT images showed a retinal detachment in the conus area of five eyes including four eyes without contractile movements of the optic disc and one eye with contractile movements. A retinal break was found in two eyes, and all five eyes had an abnormal communication between the subarachnoid space and the subretinal space. SD-OCT did not show differences between contractile and noncontractile movements in morning glory syndrome. Retinal detachments in morning glory syndrome are generally described to have abnormal communication between the subretinal and subarachnoid or vitreous compartments. Myopia-like retinoschisis and retinal detachments without any evidence of a retinal break were suggested to result from tissue stretching around the peripapillary conus in morning glory syndrome. Lee et al[47] reported that SS-OCT and SD-OCT were useful methods to evaluate the bottom of the cavity for differential types of excavated optic disc anomalies of morning glory syndrome, optic disc coloboma, and peripapillary staphyloma.

Ho et al[48] evaluated five eyes of five consecutive patients with morning glory syndrome with a retinal detachment. SD-OCT detected a slit-like break at the margin of excavation in four of five eyes and four eyes with the breaks underwent pars plana vitrectomy, gas injection, and postoperative laser photocoagulation. In the one eye in which no retinal break could be detected by SD-OCT, the retina was reattached after pars plana vitrectomy and removal of gel-like tissue. The retina was reattached in all five eyes during the 3–50-month (average 28-month) follow-up period. Postoperative OCT showed a closure of the retinal breaks at the margin of the excavation. Optical coherence tomography was able to detect subtle slit-like breaks at the margin of the excavation in the retinal detachment in the morning glory syndrome. Nagasawa et al[49] reported a probable subarachnoid space and its direct communication with the vitreous cavity in a patient with morning glory syndrome.

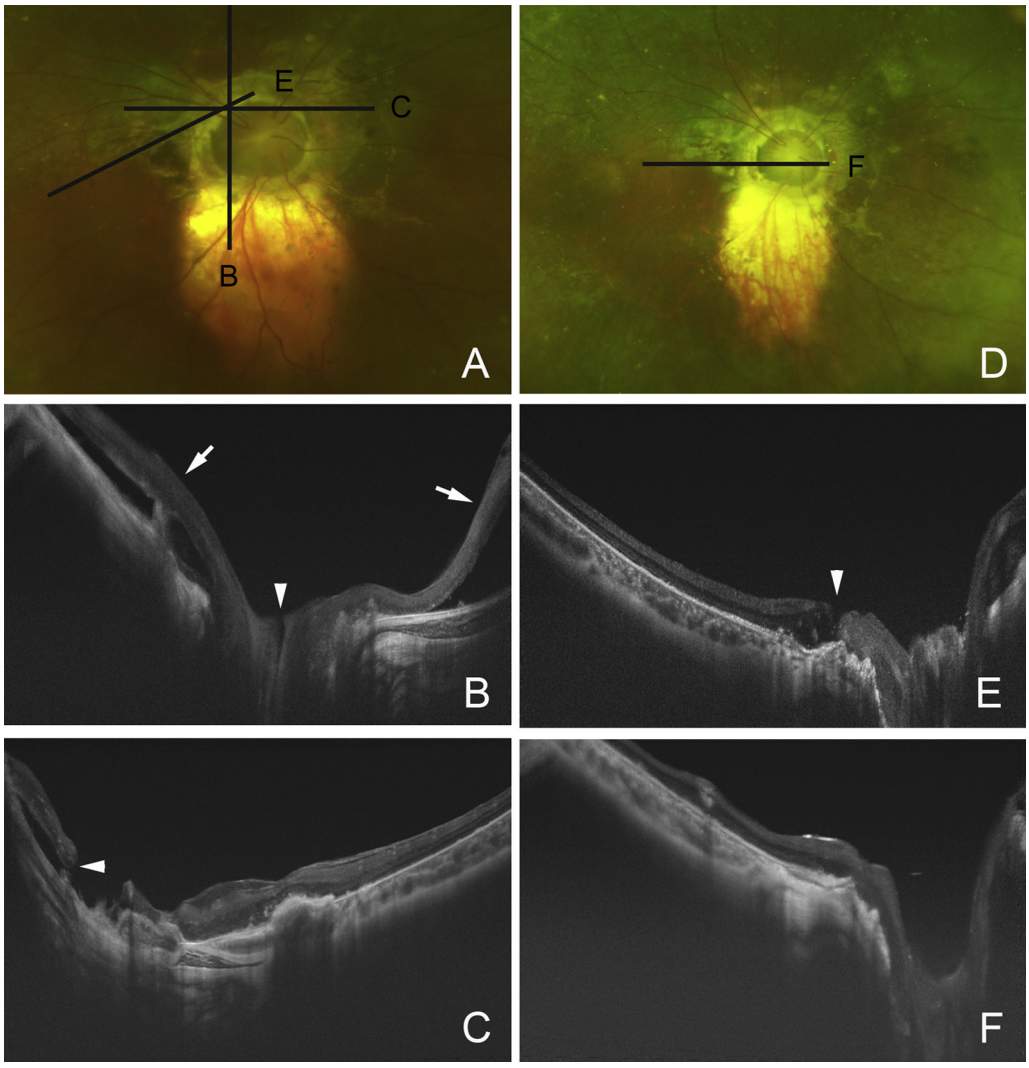

Fig. 7. Pre- and postoperative Optos image and swept-source optical coherence tomography (SS-OCT) images of a patient with the morning glory syndrome in a 14-year old boy. (A) Preoperative Optos image showing a total retinal detachment except in the supratemporal quadrant. Black lines indicate the scan lines of cross section of the SS-OCT images of Figures B and C (before initial surgery), and E (after initial surgery); (B) vertical SS-OCT image shows superior and inferior retinal detachments (arrows) and a direct communication between vitreous cavity and possible subarachnoid space; (C) horizontal SS-OCT image shows small retinal break at the edge of the peripapillary atrophy around the excavated optic disc; (D) postoperative Optos image showing retinal reattachment after the second surgery with silicone oil tamponade; (E) oblique SS-OCT image shows macular hole which was revealed after the initial surgery; (F) vertical SS-OCT image shows closure of macular hole after the second surgery with silicone oil tamponade and internal limiting membrane peeling.

2. Conclusions

The introduction and use of SS-OCT in eyes with congenital optic disc anomalies has led to significant improvements in the evaluation of the pathology of congenital optic disc anomalies. Treatments for retinal complications associated with congenital optic disc anomalies are varied and depend on the specific imaging findings. Further analyses by SS-OCT for congenital optic disc anomalies may enable clinicians to select treatments that are more appropriate for the pathological conditions.

References

1. Bartz-Schmidt KU, Heimann K. Pathogenesis of retinal detachment associated with morning glory disc. *Int Ophthalmol*. 1995;19:35–38.
2. Coll GE, Chang S, Flynn TE, Brown GC. Communication between the subretinal space and the vitreous cavity in the morning glory syndrome. *Graefes Arch Clin Exp Ophthalmol*. 1995;233:441–443.
3. Gass JD. Serous detachment of the macula. Secondary to congenital pit of the optic nervehead. *Am J Ophthalmol*. 1969;67:821–841.
4. Brown GC, Shields JA, Goldberg RE. Congenital pits of the optic nerve head. II. Clinical studies in humans. *Ophthalmology*. 1980;87:51–65.
5. Taylor D. Developmental abnormalities of the optic nerve and chiasm. *Eye (Lond)*. 2007;21:1271–1284.
6. Lincoff H, Kreissig I. Optical coherence tomography of pneumatic displacement of optic disc pit maculopathy. *Br J Ophthalmol*. 1998;82:367–372.
7. Huang D, Swanson EA, Lin CP, et al. Optical coherence tomography. *Science*. 1991;254:1178–1181.
8. Drexler W, Fujimoto JG. State-of-the-art retinal optical coherence tomography. *Prog Retin Eye Res*. 2008;27:45–88.
9. Choma MA, Hsu K, Izatt JA. Swept source optical coherence tomography using an all-fiber 1300-nm ring laser source. *J Biomed Opt*. 2005;10:44009.
10. Ohno-Matsui K, Akiba M, Moriyama M, Ishibashi T, Tokoro T, Spaide RF. Imaging retrobulbar subarachnoid space around optic nerve by swept-source optical coherence tomography in eyes with pathologic myopia. *Invest Ophthalmol Vis Sci*. 2011;52:9644–9650.
11. Ohno-Matsui K, Akiba M, Ishibashi T, Moriyama M. Observations of vascular structures within and posterior to sclera in eyes with pathologic myopia by swept-source optical coherence tomography. *Invest Ophthalmol Vis Sci*. 2012;53:7290–7298.
12. Ohno-Matsui K, Akiba M, Moriyama M, Ishibashi T, Hirakata A, Tokoro T. Intrachoroidal cavitation in macular area of eyes with pathologic myopia. *Am J Ophthalmol*. 2012;154:382–393.
13. Ohno-Matsui K, Shimada N, Akiba M, Moriyama M, Ishibashi T, Tokoro T. Characteristics of intrachoroidal cavitation located temporal to optic disc in highly myopic eyes. *Eye (Lond)*. 2013;27:630–638.
14. Spaide RF, Akiba M, Ohno-Matsui K. Evaluation of peripapillary intrachoroidal cavitation with swept source and enhanced depth imaging optical coherence tomography. *Retina*. 2012;32:1037–1044.
15. Takayama K, Hangai M, Kimura Y, et al. Three-dimensional imaging of lamina cribrosa defects in glaucoma using swept-source optical coherence tomography. *Invest Ophthalmol Vis Sci*. 2013;54:4798–4807.
16. Yoshikawa M, Akagi T, Hangai M, et al. Alterations in the neural and connective tissue components of glaucomatous cupping after glaucoma surgery using swept-source optical coherence tomography. *Invest Ophthalmol Vis Sci*. 2014;55:477–484.
17. Wang B, Nevins JE, Nadler Z, et al. Reproducibility of *in-vivo* OCT measured three-dimensional human lamina cribrosa microarchitecture. *PLoS One*. 2014;9:e95526.
18. Leitgeb R, Hitzenberger C, Fercher A. Performance of Fourier domain vs. time domain optical coherence tomography. *Opt Express*. 2003;11:889–894.
19. Sull AC, Vuong LN, Price LL, et al. Comparison of spectral/Fourier domain optical coherence tomography instruments for assessment of normal macular thickness. *Retina*. 2010;30:235–245.
20. de Boer JF, Cense B, Park BH, Pierce MC, Tearney GJ, Bouma BE. Improved signal-to-noise ratio in spectral-domain compared with time-domain optical coherence tomography. *Opt Lett*. 2003;28:2067–2069.
21. Spaide RF, Koizumi H, Pozzoni MC. Enhanced depth imaging spectral-domain optical coherence tomography. *Am J Ophthalmol*. 2008;146:496–500.
22. Imamura Y, Fujiwara T, Margolis R, Spaide RF. Enhanced depth imaging optical coherence tomography of the choroid in central serous chorioretinopathy. *Retina*. 2009;29:1469–1473.
23. Itakura H, Kishi S, Li D, Akiyama H. Observation of posterior precortical vitreous pocket using swept-source optical coherence tomography. *Invest Ophthalmol Vis Sci*. 2013;54:3102–3107.
24. Schaal KB, Pang CE, Pozzoni MC, Engelbert M. The premacular bursa's shape revealed in vivo by swept-source optical coherence tomography. *Ophthalmology*. 2014;121:1020–1028.
25. Kishi S, Shimizu K. Posterior precortical vitreous pocket. *Arch Ophthalmol*. 1990;108:979–982.
26. Worst JG. Cisternal systems of the fully developed vitreous body in the young adult. *Trans Ophthalmol Soc U K*. 1977;97:550–554.
27. Worst J. Extracapsular surgery in lens implantation (Binkhorst lecture). Part iv. Some anatomical and pathophysiological implications. *J Am Intraocul Implant Soc*. 1978;4:7–14.
28. Kishi S, Hagimura N, Shimizu K. The role of the premacular liquefied pocket and premacular vitreous cortex in idiopathic macular hole development. *Am J Ophthalmol*. 1996;122:622–628.
29. Itakura H, Kishi S, Li D, Nitta K, Akiyama H. Vitreous changes in high myopia observed by swept-source optical coherence tomography. *Invest Ophthalmol Vis Sci*. 2014;55:1447–1452.
30. Yokoi T, Toriyama N, Yamane T, Nakayama Y, Nishina S, Azuma N. Development of a premacular vitreous pocket. *JAMA Ophthalmol*. 2013;131:1095–1096.
31. Li D, Kishi S, Itakura H, Ikeda F, Akiyama H. Posterior precortical vitreous pockets and connecting channels in children on swept-source optical coherence tomography. *Invest Ophthalmol Vis Sci*. 2014;55:2412–2416.
32. Georgalas I, Ladas I, Georgopoulos G, Petrou P. Optic disc pit: A review. *Graefes Arch Clin Exp Ophthalmol*. 2011;249:1113–1122.
33. Hirakata A, Hida T, Wakabayashi T, Fukuda M. Unusual posterior hyaloid strand in a young child with optic disc pit maculopathy: intraoperative and histopathological findings. *Jpn J Ophthalmol*. 2005;49:264–266.
34. Ohno-Matsui K, Hirakata A, Inoue M, Akiba M, Ishibashi T. Evaluation of congenital optic disc pits and optic disc colobomas by swept-source optical coherence tomography. *Invest Ophthalmol Vis Sci*. 2013;54:7769–7778.
35. Katome T, Mitamura Y, Hotta F, Mino A, Naito T. Swept-source optical coherence tomography identifies connection between vitreous cavity and retrobulbar subarachnoid space in patient with optic disc pit. *Eye (Lond)*. 2013;27:1325–1326.
36. García-Arumí J, Guraya BC, Espax AB, Castillo VM, Ramsay LS, Motta RM. Optical coherence tomography in optic pit maculopathy managed with vitrectomy-laser-gas. *Graefes Arch Clin Exp Ophthalmol*. 2004;242:819–826.
37. Hirakata A, Okada AA, Hida T. Long-term results of vitrectomy without laser treatment for macular detachment associated with an optic disc pit. *Ophthalmology*. 2005;112:1430–1435.
38. Hirakata A, Inoue M, Hiraoka T, McCuen 2nd BW. Vitrectomy without laser treatment or gas tamponade for macular detachment associated with an optic disc pit. *Ophthalmology*. 2012;119:810–818.
39. Shukla D, Kalliath J, Tandon M, Vijayakumar B. Vitrectomy for optic disk pit with macular schisis and outer retinal dehiscence. *Retina*. 2012;32:1337–1342.
40. Jain N, Johnson MW. Pathogenesis and treatment of maculopathy associated with cavitary optic disc anomalies. *Am J Ophthalmol*. 2014;158:423–435.
41. McDonald HR, Lewis H, Brown G, Sipperley JO. Vitreous surgery for retinal detachment associated with choroidal coloboma. *Arch Ophthalmol*. 1991;109:1399–1402.
42. Hanneken A, de Juan Jr E, McCuen 2nd BW. The management of retinal detachments associated with choroidal colobomas by vitreous surgery. *Am J Ophthalmol*. 1991;111:271–275.
43. Hotta K, Hirakata A, Hida T. Retinoschisis associated with disc coloboma. *Br J Ophthalmol*. 1999;83:124.
44. Hotta K, Hirakata A, Hida T. The management of retinal detachments associated with choroidal colobomas by vitrectomy with cyanoacrylate retinopexy. *Jpn J Ophthalmol*. 1998;42:323–326.
45. Pal N, Azad RV, Sharma YR. Long-term anatomical and visual outcome of vitreous surgery for retinal detachment with choroidal coloboma. *Indian J Ophthalmol*. 2006;54:85–88.
46. Cennamo G, de Crecchio G, Iaccarino G, Forte R, Cennamo G. Evaluation of morning glory syndrome with spectral optical coherence tomography and echography. *Ophthalmology*. 2010;117:1269–1273.
47. Lee KM, Woo SJ, Hwang JM. Evaluation of congenital excavated optic disc anomalies with spectral-domain and swept-source optical coherence tomography. *Graefes Arch Clin Exp Ophthalmol*. 2014;252:1853–1860.
48. Ho TC, Tsai PC, Chen MS, Lin LL. Optical coherence tomography in the detection of retinal break and management of retinal detachment in morning glory syndrome. *Acta Ophthalmol Scand*. 2006;84:225–227.
49. Nagasawa T, Mitamura Y, Katome T, Nagasato D, Tabuchi H. Swept-source optical coherence tomographic findings in morning glory syndrome. *Retina*. 2014;34:206–208.